



## Synthesis and characterization of sdc-bcs composite electrolyte for solid oxide fuel cells

A. Senthil Kumar <sup>1</sup>

1. Department of Physics, PSG College of Technology, Peelamedu, Coimbatore-641004, TN, INDIA.

Received 22 Jun 2016,  
Revised 21 Oct 2016,  
Accepted 25 Oct 2016

### Keywords

- ✓ Sintering Method;
- ✓ Doped barium cerate;
- ✓ Nanocomposite;
- ✓ Electrolyte;
- ✓ Solid Oxide Fuel cell.

A. Senthil Kumar  
[senthu.ramp@gmail.com](mailto:senthu.ramp@gmail.com)  
+91 9842089556

### Abstract

Samarium doped barium cerate (SDC-BCS) solid solution is synthesized through coprecipitation technique. A SDC-BCS perovskite oxide ion conducting nanocomposite electrolyte is studied with respect to its thermal, structural, morphology and conductivity performance. The crystal structure and microstructure of composite is analyzed using XRD and SEM techniques respectively. The crystal structure of as prepared composite powder is identified as cubic perovskite with orthorhombic distortions occurred at 900°C (TGA). From TEM analysis, the particle size is found to be around 27nm, uniform in size, shape. SEM analysis reveals that the existence of dual phase, free from pores and homogenous distribution of SDC-BCS phase in the composite. The enforcement of the specific sintering method (microwave) allows the preparation of dense nanocomposite with the development of dual phase to get improved ionic conductivity for niche fuel cell applications.

## 1. Introduction

Solid oxide fuel cells (SOFCs) attracted a great deal of consideration among the promising fuel cell systems for energy conversion. In SOFC, electrolyte plays a vital role in increasing the efficiency of energy conversion. The main hurdle for fuel cell is its higher operating temperature (1000°C) which results in design limitation and higher fabrication cost. Current trend in SOFC have attracted the young researcher to develop a suitable oxygen ion conducting solid electrolytes for electrochemical energy conversion with high efficiency, low cost, more sustainable and environmentally friendly in nature. In SOFC electrolyte is considered as a main component with high performance rate by means of high oxide ion diffusion for the conversion of required ionic conductivity (0.1S cm<sup>-1</sup>). Anode and cathode are the supporting electrodes, where the half cell reaction takes place. So far 8 mol% of Yttria Stabilized Zirconia (YSZ) has been a considered as a potential candidate for high ionic conductivity with negligible electronic conduction at 1000°C [1]. YSZ has shown sustained ionic conduction in both oxidizing and reducing atmosphere. But the main problem associated with these Zirconia based electrolyte is its thermal mismatch, instability at high temperature and higher cost which limits its niche commercial requirements.

In order to overcome the above stated problems, the operating temperature of solid electrolyte must be reduced to intermediate temperature (600-800°C) [2, 3]. Ceria based electrolytes with fluorite structure have become a possible oxygen ion conducting electrolyte to replace Yttria Stabilized Zirconia (YSZ) with high ionic conductivity at intermediate temperature (600°C-800°C). But pure ceria is not a good oxygen conductor. Doping of an aliovalent cation into ceria lattice is an effective approach to facilitate the creation of oxygen vacancies thereby improving the ionic conductivity. However, these doped ceria materials exhibits its low open cell voltage(OCV) with partially increased electronic conduction and acts as a n-type conductor due to the reduction of Ce<sup>4+</sup> to Ce<sup>3+</sup> [4, 5]. That is the formation of oxide defect at high temperature results in instability of oxygen partial pressure during fuel cell operation and in turn reduces its OCV [6,7]. Another class of pervoskite type oxide (ABO<sub>3</sub>) structures such as barium cerate, strontium cerate, barium zirconate are considered as best solid electrolytes [8,9] with required high ionic conductivity at intermediate temperature with the reduced electronic conduction. But, these undoped BaCeO<sub>3</sub> Pervoskite structure shows some instability in CO<sub>2</sub> atmosphere, due to the formation of BaCO<sub>3</sub>, which in turn provide poor mechanical strength and to decrease the

ionic conductivity of the electrolyte [10, 11]. Hence doped barium cerate based materials such as samarium or gadolinium with fluorite-pervoskite structured can overcome the above stated individual problems and are highly preferred as solid electrolyte for fuel cell application.[12,13]. The presence of doped barium cerate (BCS) as second phase in composite will prevent the internal leakage of electrons caused by the reduction mechanism occurred in first phase called samarium doped ceria phase (SDC) and ultimately improve the open circuit voltage of the fuel cell [14]. In the present research work, samarium doped barium cerate based SDC-BCS composite electrolyte is prepared as an electrolyte for high ionic conductivity at BCS phase and low electronic conduction in SDC phase at intermediate operating temperature.

## 2. Experimental work:

### 2.1 SDC-BCS Powder Synthesis:

The Samarium doped barium cerate (SDC-BCS) composite electrolyte powder is successfully synthesized through co precipitation method with  $(1-x)\text{Ce}_{0.8}\text{Sm}_{0.2}\text{O}_{2-\delta} - x\text{BaCe}_{0.8}\text{Sm}_{0.2}\text{O}_{3-\delta}$  stoichiometry, where  $x= 0.1$  mole fraction. Cerium nitrate, samarium nitrate and barium nitrate (99.5% pure) powders purchased from Sigma–Aldrich are dissolved in 50 ml of distilled water in a beaker until the salt gets dissolved completely to forms their respective nitrates. The weight ratio for SDC-BCS composite powder with 10 mol% of Ba content is shown in Table.1.

Table 1 Weight ratio for Ba10CS compositions

Sample Name	Barium Nitrate in mol fraction	Cerium Nitrate in mol fraction	Samarium Nitrate in mol fraction
Ba10CS	0.1	0.8	0.2

Three solutions are poured in a burette one by one and added together in a beaker drop-by-drop slowly with continuous stirring at 500 rpm in a magnetic stirrer. Ammonium hydroxide solution is added into the mixture to maintain the pH >10. By the addition of  $\text{NH}_4\text{OH}$ , the mixture is precipitated out as hydroxides of Cerium, Barium, and Samarium and kept on a magnetic stirrer with 1000 rpm for 30 minutes for homogeneity. In order to obtain the gel, the mixture is then added with 10% of PEG (Poly Ethylene Glycol) acts as a complexation agent and again stirred well for about 30 minute to improve the formation of green body solid solution [15]. To dry out the gel, the precipitate is dried in hot air oven maintained at  $95^\circ\text{C}$  for 12 hours. The obtained flakes are kept in furnace at  $400^\circ\text{C}$  for 2 hr to get the dry powder. The dry powder is again grained well and calcined up to  $900^\circ\text{C}$  to obtain the required SDC-BCS composite matrix with dual phase.

### 2.2 SDC-BCS Pellet Preparation:

The dense SDC-BCS composite pellets are prepared from the precursor powder by uniaxial pressing with 15MPa using a steel die of 12 mm diameter. Before pressing into pellets, the as prepared powder is mixed well with 1 % of Poly vinyl alcohol (PVA) as a binder to get the well compact green pellet. The addition of PVA to the precursor powder can ultimately improve the good sintering ability and in turn increase the strength of the pellet. The well compacted pellets are taken in alumina boat for sintering using microwave furnace. In microwave, the sintering procedure is carried out for 20 min at heating rate of  $45^\circ\text{C}$  per min. Hence, disc shaped SDC-BCS composites electrolyte is prepared.

### 2.3 Composite Materials Characterization:

The prepared SDC-BCS composite electrolyte powder and pellets are physically characterized. Thermal analysis (TGA) is carried out with the help of Netzsch, Germany, NETZSCH STA 449F/3 Instruments to identify the calcination temperature of the as prepared powder. XRD analysis is carried out to determine the crystallinity and the phase purity of the as-prepared green powder. The structural analyses for the synthesized powders and sintered pellets are characterized through Shimadzu powder X-ray diffraction analyzer, in nickel filtered  $\text{Cu-K}\alpha$  ( $\lambda = 0.15418$  nm) radiation. The scans ranged between  $20^\circ < 2\theta < 90^\circ$  with an interval of  $0.1^\circ\text{min}^{-1}$ . The particle size distribution is examined and identified through Transmission electron microscopy (TEM, JEM-2010) along with an energy- dispersive X-ray spectroscopy (EDS) system. Scanning electron microscopy (SEM, JEOL JSM-6700F) is employed to examine the surface morphology of the powders and its microstructures development. Conductivity measurement is carried out for all the composites using Novo control GmbH Alpha-A high-resolution electrochemical impedance analyzer. Impedance measurement is performed to know the electrical behavior of composite electrolyte. The total conductivity of the composite is obtained from the impedance spectra. Platinum electrodes are used with homemade sample holder.

### 3. Results and discussions

#### 3.1 Thermal Analysis for powder sample:

Thermogravimetric analysis (TGA) is used to measure the mass loss (%) of powder sample with increase in temperature. TG analysis is mainly used to determine the temperature of phase formation and to study the decomposition reaction occurred in the sample. The collective Thermal investigation (Thermo gravimetric Analysis-TGA) is carried out for the as prepared Ba10CS powder for determining its calcination temperature. The TGA thermogram is recorded under nitrogen atmosphere at an invariable heating rate of 10°C per minute from room temperature to 1100°C.

Figure 1 (a-c) exhibits the TGA thermograms of as prepared powder with 10 mol% of Ba content. TGA patterns are provided simultaneously to understand the origin of the endothermic peaks and associated weight loss. The loss is clearly noticed in TGA pattern. The percentage of weight loss for all the three samples falls between 2 to 4 wt%. The gradual decrease in weight is observed till 500°C and followed by a steep behavior till 600°C (Figure.1.a, b). The weight loss in this temperature range is attributed to the loss of organic compound present in the as prepared powder. The presence of second endothermic peak present at 550°C confirms the study. Noteworthy, the decomposition of nitrates takes place between 550°C to 700°C as studied in previous available literature [15]. The presence of third endothermic peak at 870°C with 2% weight loss in all the three samples indicates the decomposing of left over barium nitrate into BaO for favoring the formation of BCS phase. Figure 1c clearly depicts that the percentage of weight loss is only 2%. It is understood from the above studies that the formation of BCS phase occurs at 900°C. However, the formation of SDC phase is not known from this study. It is understood from the literature that the formation of SDC phase for micron sized particles can occur at 700°C [16]. In this case, the evidence of formation of SDC phase may be over shadowed by the weight loss at various stages.

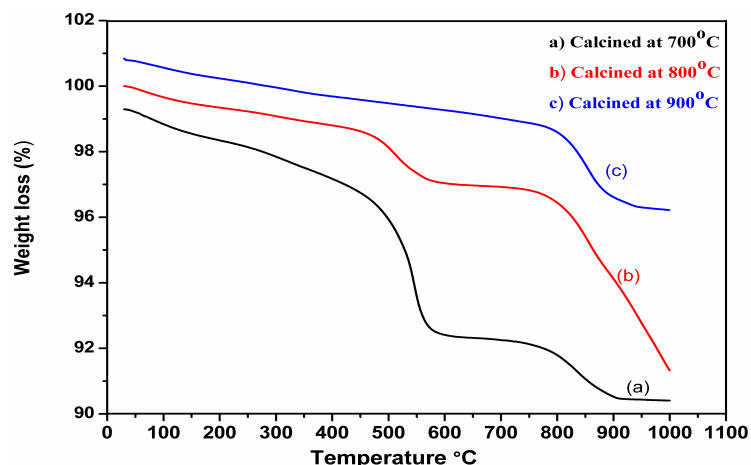


**Figure.1** Thermal-analysis for Ba10CS composite powder calcined at various temperatures.

In order to determine the phase formation temperature for SDC and ascertain the formation of BCS phase, the as prepared powders with 10 mol% of Ba content (Ba10CS) is calcined at 700°C, 800°C and 900°C for 4 hours.

#### 3.2 XRD Studies for Powder sample:

X-ray diffraction analysis is performed for the as prepared powder calcined at three different temperatures say 700°C, 800°C and 900°C respectively for about 3 hours shown in Figure.2. The structural characteristics, the phase purity and the crystal lattice parameters are determined at room temperature. The XRD results indicated that the powder calcined at 900°C have shown the complete dissolution of the dopant into barium cerate lattice and leads to the formation of dual phase with fluorite- perovskite-type structure of Pmcn space group. In order to study the formation of SDC-BCS composites structure by the reaction process occurred through co precipitation. One can clearly see the variation of diffraction pattern for the as prepared powder, while increase in calcination temperature. As the calcinations temperature is increased from 700°C to 900°C, more diffraction peaks are emerged and are attributed to the formation of BaO from Ba(NO<sub>3</sub>)<sub>2</sub>. When the calcination temperature of the powder increases, the characteristics peak position at 23°92' corresponds to BaCO<sub>3</sub> phase entirely disappeared due to the formation of samarium doped BaCeO<sub>3</sub> phase. The fluorite and perovskite structure is fashionably produced respectively for SDC and BCS powder calcined at 900°C [28]. The diffraction peaks corresponds to SDC phase along (111) plane and BCS phase along (020) plane are clearly displayed and no impure phases are observed for SDC-BCS composite, which indicates that SDC phase has good chemical compatibility with BCS phase in composite electrolyte powder.

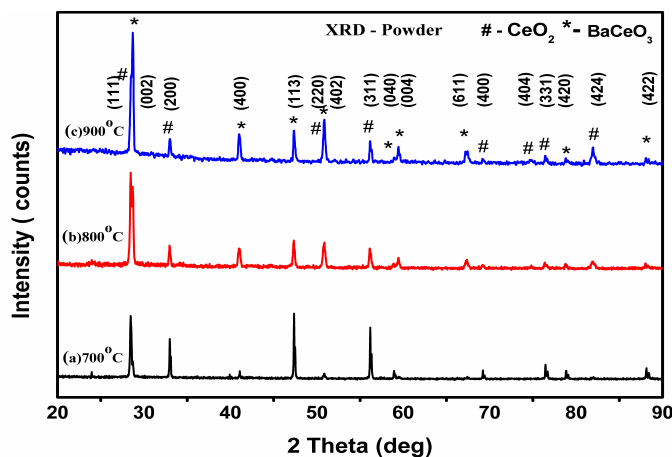
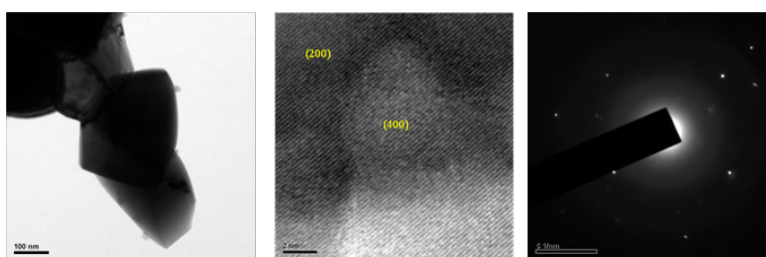


**Figure.2** Structural analysis for SDC-BCS powder calcined at various temperatures for 4 hours

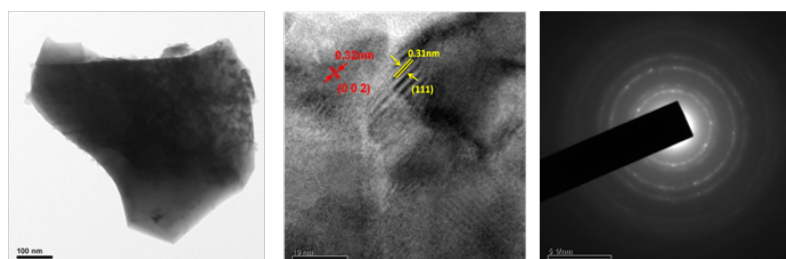
The high intense peak present at  $28.42^\circ$  correspond to SDC phase and  $28.68^\circ$  for BCS phase. The existence of these two phases confirms that most of the grains are oriented at (111) plane and (002) plane of both the SDC and BCS phases respectively. The gradual enhancement in the volume of BCS phase i.e. barium cerate phase is observed as the calcination temperature increases in the step of  $100^\circ\text{C}$ .

### 3.3 HRTEM Analysis for Powder sample:

HRTEM analysis is carried out for Ba10CS powder calcined at  $700^\circ\text{C}$  and  $900^\circ\text{C}$  to gain the information on particle size distribution, shape, crystal structure and variation of particle size with increase in the calcination temperature of as prepared powder. The HR-TEM image displayed in Figure. 3a(i) and 3b(i) confirms the distribution of particle and the presence of nanocrystalline variations in the powder processed through chemical route method. The JEOL JEM 2100 High Resolution Transmission Electron Microscope (HRTEM) is used to analysis the samples. The nanoparticle are found to be around 27nm in size estimated by HR-TEM and are similar to the values calculated from XRD results, evidencing the development of SDC-BCS nanocomposite powder processed through chemical route. The lattice spacings of 0.31nm and 0.32 nm shown in Figure 3a(ii) and 3b(ii) corresponds to the (111) and (002) crystal plane of doped ceria (SDC) and doped barium cerate (BCS) respectively. The presence of stoichiometric  $\text{BaCe}_{0.8}\text{Sm}_{0.2}\text{O}_{1.9-\delta}$  phase is verified by EDS micro analysis as shown in Figure 3a(iii), 3b(iii) and confirms that co precipitation method lead to the complete precipitation of Ce and Sm cations in barium cerate lattice and resulted in the formation of the SDC-BCS solid solution. The existence of both the phase confirms the composite nature of the as prepared powder [17].



**Figure:3a** High resolution TEM images (i) Particle size (ii) Nano scale and (iii) SAED pattern of Ba10CS powders calcined at  $700^\circ\text{C}$  for 4 h



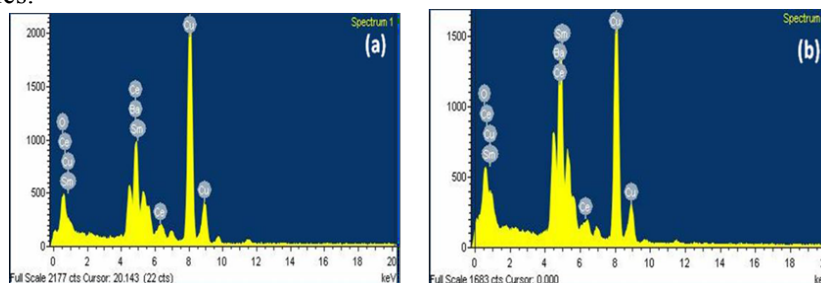
**Figure:3b** High resolution TEM images (i) Particle size (ii) Nano scale and (iii) SAED pattern of Ba10CS powders calcined at  $900^\circ\text{C}$  for 4 h

Figure 3a, 3b clearly shows a high resolution TEM micrograph of the nano-particles calcined at 700°C and 900°C. Good crystalline state and crystalline faces can also be observed from the SAED patterns of the sample calcined at 900°C which confirm the presence of crystalline nanoparticles or nanocrystallinity of the material. Strong and bright reflections are observed in SAED patterns in Figure 3b(ii) and are in good agreement with the XRD results. The ring pattern confirms that the as prepared powder is in nanometer size. From the optical imaging analysis, the average distribution of particle in the SDC-BCS powder is determined qualitatively using the imaging software. The variation of particle size between 20nm to 27nm for SDC-BCS powder is studied from TEM image. The average particle size and the range of size distribution while increasing the calcination temperature is shown in Table.2.

**Table. 2** Variation of particle size with increase in calcination temperature for Ba10CS powder

Sample Name	Calcination Temperature (°C)	Average particle size (nm)
Ba10CS	700	18
	900	27

As the particle size is lesser than 30 nm, it is expected to have low sintering temperature and soaking time [18,29]. The existence of nanoparticle in the form of composite play an important role in the densification behavior of ceramics.



**Figure.4.** EDS spectrum of SDC-BCS powder calcined at (a) 700°C and 900°C

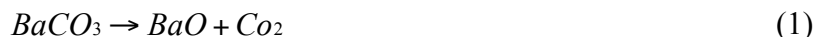
The Energy dispersive spectrum (EDS) of Ba10CS sample is shown in Figure.4. The solid solution prepared through this co precipitation method leads to the complete precipitation of  $\text{Sm}^{3+}$  ions in  $\text{BaCeO}_3$  phase. The spectrum analysis the weight and atomic percentage of all the elements present in the compound. From the EDS measurement, it is observed that the presence of Samarium, Cerium and barium in the compound with no other elements [19,30]. No evident pattern for residual impurities is observed in the as prepared SDC-BCS powder. The EDS result confirms that the method of process and the calcination temperature of electrolyte powder is are more sufficient to produce the nano composite matrix with dual phase formation.

### 3.4 XRD Studies for SDC-BCS Pellet:

The structural investigation is carried out to know the effect of sintering temperature for SDC-BCS pellet sintered at 1300°C and 1400°C for 20 min through microwave sintering. Figure.5 shows the XRD pattern for SDC phase, BCS phase and samarium doped barium cerate SDC-BCS dual phase. The XRD patterns of pellet sintered at 1300°C and 1400°C for 20 minutes in air with programmed heating rate of 45°C per minute and cooling rate of 10°C per minute using the microwave furnace. The existences of cubic fluorite structure for SDC phase and orthorhombic perovskite structure for BCS phase is observed and shown Figure 5 (c) & (d). The XRD result confirms the formation of matrix phase for the pellets sintered at 1300°C and 1400°C. The presence of major diffraction planes (020), (400) and (402) confirms that the BCS phase is successfully retained in the composite sintered at 1400°C due to the minimum soaking time of 20 min. As the sintering temperature increase, the intensity of the peak pertaining to BCS phase increases and shows the indications of increase in volume of BCS phase in the composite. The diffraction peaks for both the phases are compared and indexed from JCPDS files No:75-0158 for SDC phase and 85-2155 for BCS phase form PCPDF WIN database. In addition, no by-product phases are observed, indicating that there is no superimposition of SDC and BCS phases and result in the formation composite with matrix phase. The intensity of peak around 28.67° for (020) plane is considered as the predominant peak for samarium doped barium cerate (BCS) phase and found to increase with

increase in sintering temperature. The gradual decrease in the peak position at 28.42° of (111) plane correspond to the samarium doped ceria phase.

The high intense peak present at 28.42° and 28.68° confirms that most of the grains are oriented at (111) plane and (020) plane of both the phases respectively. It can also be observed that the diffraction pattern with the main reflexes are at (020), (400), (402), (040), (420), (611) correspond to the barium cerate phase and the reflected peaks position at (111),(200),(220), (311), (400) corresponds to samarium doped barium cerate. The XRD pattern for SDC-BCS composite shown in Figure.5 represent that the formation of BaCe<sub>1-x</sub>Sm<sub>x</sub>O<sub>3-δ</sub> doped barium cerate phase and is highly pronounced with increase in sintering temperature of the composite by following the reaction mechanism (2).



The formation of BCS phase formation with lattice parameters a = 8.753, b= 6.244 , c=6.231 are in good agreement the values earlier reported [ 20,21,28 ]. The Corresponding d-spacing values are calculated from the equation (3):

$$\frac{1}{d^2} = \frac{h^2}{a^2} + \frac{k^2}{b^2} + \frac{l^2}{c^2} \quad (3)$$

The crystalline size is calculated from the Scherer's formula (equation.4) for the high intense peak and found to increase from 30nm to 32nm. It is clearly observed that with an increase in sintering temperatures, all the peaks become sharper and this is an indication for the increase in the particle size.

$$D = \frac{0.9\lambda}{\beta \cos \theta} \quad (4)$$

Hence, from this structural analysis, it is inferred that the as prepared powder sintered at 1400°C can influence the formation of composite structure with individual SDC and BCS phase, obtained through chemical co precipitation method and co fired by means of microwave sintering as shown in equation (1).

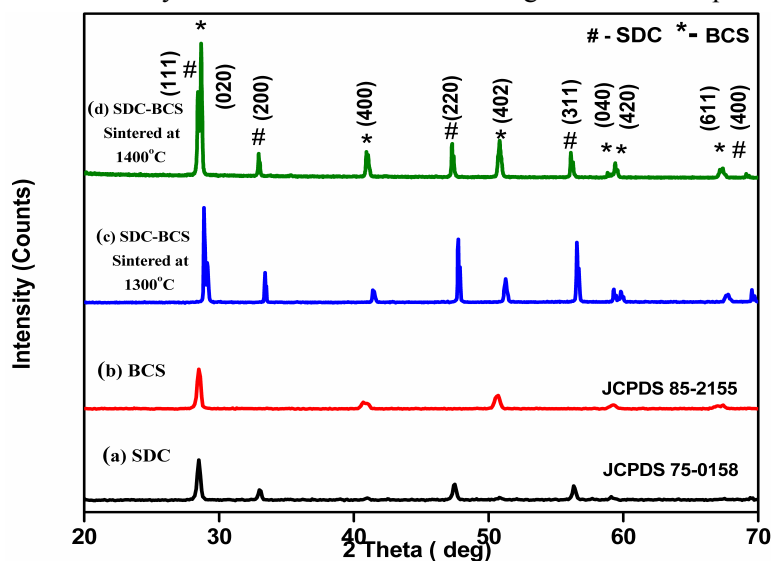


**Figure:5 Structural analysis of Ba10CS pellet sintered at 1300°C and 1400°C for 20mins**

The lattice parameter and unit cell volume for both the phases is calculated from XRD data. The corresponding lattice parameters, unit cell volume of Ba10CS composite is calculated from equation (3) and are listed in Table-3 with comparison to the earlier reported values and found to match exactly noteworthy at lower sintering temperature, which reveals that these SDC-BCS phase is successfully retained at 1400°. All the major peak, d-spacing values are in well agreement with the JCPDS data of Reference code: 85-2155 [13]. Density values for both the samples are measured to be 92% and 96% respectively using the normal geometric calculations (not shown).

### 3.5 SEM Analysis for SDC-BCS Pellet:

SEM analysis is carried out to observe the morphology of SDC-BCS composite electrolytes sintered at 1300°C and 1400°C. As expected, the composite electrolyte exhibited uniform distribution of SDC and BCS grains. It can be seen from Figure.6 that the composite exhibits the average grain size of 2-4 μm and are quite dense in

nature without having any connected pores. The calculated porosity from SEM image is found to be ~12%. The observed morphology is mainly recognized as SDC- BCS grains in the form of composite matrix [22].

**Table ; 3** Unit cell parameters for composite pellets sintered at 1400°C for 20 mins.

Method of synthesis	Temperature of Synthesis (K)	Type of structure	Unit cell parameters			Unit cell volume	Ref.
			a	b	c		
Sintering	1673- 1723	orthorhombic	8.791	6.252	6.227	342.24	[16]
annealing	1620-1670	orthorhombic	8.774	6.215	6.233	339.88	[17]
BaCe <sub>0.9</sub> Gd <sub>0.1</sub> O <sub>3</sub>	1600-1650	orthorhombic	8.770	6.221	6.244	340.66	[18]
BaCe <sub>0.8</sub> Gd <sub>0.2</sub> O <sub>2</sub>	1500	orthorhombic	8.816	6.233	6.180	338.8	[19]
Ba10CG	1500-1550	orthorhombic	8.791	6.242	6.212	340.8	[15]
Ba40CG	1550-1550	orthorhombic	8.774	6.244	6.203	339.8	[15]
Ba10CS	1400	orthorhombic	8.753	6.244	6.231	340.94	This Work
Ba10CS	1300	orthorhombic	8.796	6.239	6.212	340.54	This Work

The SEM image shows no porosities, thus avoiding the possible effect of these on the impedance response of the composites. Figure 6(a) and 6(b) exhibits the distribution of two types of grain size. The observed grain size are in micron and submicron range. The micron size grain is continuous and acts as matrix. Grain boundary is well defined between the microns sized grains. The grains are almost uniform in size and perfectly packed with each other. The mean grain sizes of the pellet sintered at 1300°C and 1400°C are approximately 2µm and 4µm, respectively. The pellet sintered at 1400°C shows homogeneous distribution of submicron sized grain within the matrix and acts as reinforcement in the composites. The submicron grains are present only in the voids between the micron sized grains and thus increasing the density of the composites. From XRD studies, it is confirmed the existence of both SDC and BCS phase in the composite. Based on XRD and SEM analysis, the micron size grain is attributed as SDC phase and sub micron sized grains belong to BCS phase in the composite sintered at 1400°C [23]. The volume of BCS phase is found to increase and is consistent with the XRD results. The presence of SDC grain in composite acts as a protective layer for BCS crystalline grains as predicted [14]. Grain size increased and grain boundary decreased as sintering temperature increased from 1300°C to 1400°C and this behavior can enhance the ionic conductivity in SDC- BCS composite. When compared with the chemical stability of SDC and BCS phase individually, the presence of these two phase in SDC-BCS composites in the form of matrix can apparently improve the chemical stability of electrolyte when operated at high temperature. Thus, the existence of SDC and BCS grains are acting as a protective layer for each other.

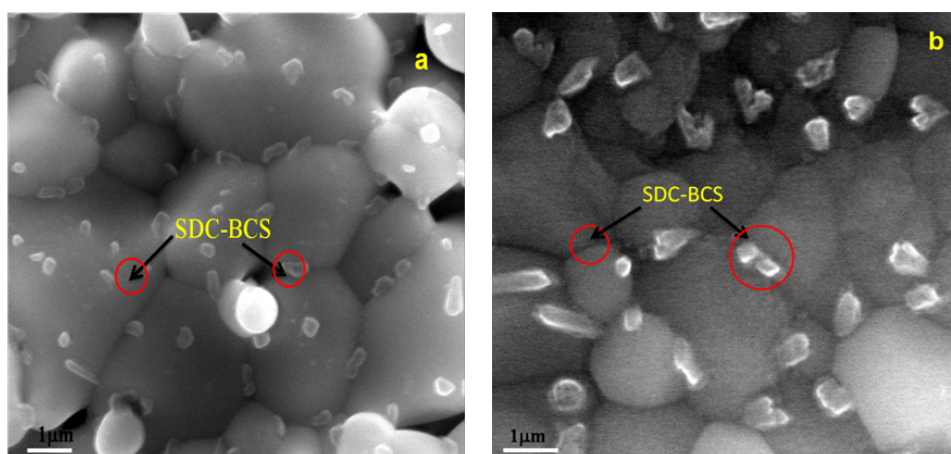


**Figure.6** Microstructural image for Ba10CS pellet sintered at (a) 1300°C and (b) 1400°C

The properties of grain and grain boundary for any polycrystalline materials are greatly influenced by the development of microstructures for studying their conductive phenomenon [24]. So a solid electrolyte sintered in the microwave can have higher ionic conductivity through smaller grains than grain boundaries because the grain boundaries are having larger resistance value than the bulk one. Hence, from this SEM analysis it is understood that the high dense pellet of two phase microstructures are grown in equal size while increasing the sintering temperature of the solid ceramic using microwave furnace in less soaking time. This SDC-BCS two-phase microstructure observed in solid electrolyte holds its good agreement with XRD two-phase predictions

[14,25]. The morphology from SEM analysis clearly shows the existence of five different component and they are SDC grains, BCS grains, grain boundary between SDC phases, grain boundary between BCS phases and grain boundary between SDC and BCS phases.

### 3.6 Impedance measurements for SDC-BCS Pellet

The Impedance measurement is carried out for Ba10CS composite electrolyte sintered at 1300°C and 1400°C respectively. The measurement is performed over the frequency range from 1Hz to 1MHz, with an applied potential of 0.1V for the temperature range between 300°C-800°C.

In addition to understand the electrical behavior of SDC-BCS composite, the electrochemical property of the pellet sintered at 1300°C and 1400°C is studied by EIS at the Open Circuit Voltage condition. The equivalent circuit of  $R_0(R_1Q_1)(R_2Q_2)(R_3Q_3)$  are used for fitting the data using EC lab Software. The Nyquist plots are fitted between the real and imaginary parts of the impedance. Figure.7 shows the Nyquist plots for SDC-BCS composite recorded at 700°C. The resistances measured at intermediate frequency semicircle are generally ascribed to grain boundary effect. The resistance of the pellet sintered at 1300°C is higher than the pellet sintered at 1400°C. The variation in resistance phenomenon is due to the change in microstructure of the composite and the effect of grain boundary diffusions.

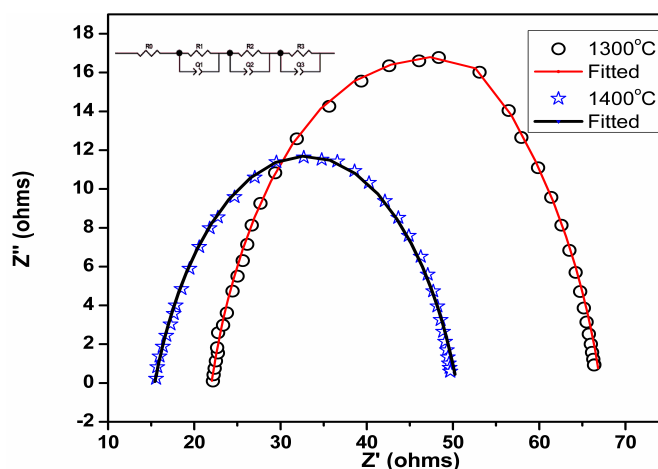


Figure.7 EI Spectrum for Ba10CS composite measured at 700°C

The cole-cole plots are fitted between the real and imaginary parts of the impedance. This plots are usually appears in the form of two semicircles, represent the different conduction mechanism occurred in the materials. From Nyquist plot as shown in Figure.7 it is observed that the radius of the semicircle decreases with increase in sintering temperature. The change in resistance with raise in temperature is mainly due to decrease in bulk resistance of the electrolyte materials and thus inferred that there is an increase in the conductivity of the composite materials

The Arrhenius plot for both the composites with increase in sintering temperature from 1300°C to 1400°C is drawn. It is well understood that the increase in BCS pervoskite phase will ultimately decrease the activation energy at low temperature as shown in Figure.8 for SDC-BCS composites materials and result in higher ionic conductivity. Hence the co existence of fluorite and pervoskite phase in SDC-BCS composite electrolyte can effectively block the leakage of electronic current through SDC phase and ultimately improves the mobility of oxygen ions through BCS phase [26].

The bulk conductivities and activation energies values are calculated using the following equations (5):

$$\sigma = \frac{L}{SR} \quad (5)$$

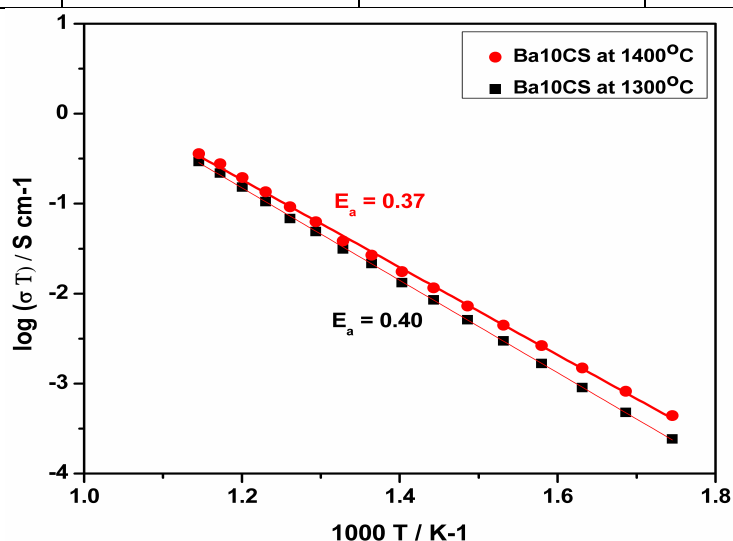
where  $\sigma$  is the conductivity, L is the thickness of the electrolyte, S is the tested electrolyte area, R is the corresponding resistance of the electrolyte, and the activation energy corresponds to the conductivity of the electrolyte is calculated from the linear fit of the Arrhenius curves using the following Arrhenius equation.

$$\sigma T = A \exp\left(-\frac{E_a}{kT}\right) \quad (6)$$

T is the temperature in Kelvin, A is the pre-exponential factor,  $E_a$  is the activation energy and k is the Boltzmann constant. Here to be noticed that we considered only the total conductivity of the electrolyte at a limited temperatures of 700°C.

**Table.4** Variation of conductivity and activation energy of Ba10CS composite

Sample Name	Sintering Temperature (°C)	Conductivity (S/cm) at 700 °C	Activation Energy (eV)
Ba10CS	1300	$3.86 \times 10^{-3}$	0.40
	1400	$1.19 \times 10^{-3}$	0.37

**Figure.8.** The Arrhenius plot of Ba10CS composite electrolyte

The total conductivity for SDC-BCS composites electrolytes is the sum of the conductivity of SDC-BCS grains, grain boundary between BCS, grain boundary between SDC and grain boundary between SDC and BCS grains. The total ionic conductivity of the composites is extracted from the equivalent circuit fitted over the respective Nyquist plot. The total ionic conductivity and activation energy as a function of temperature for  $(1-x) \text{Ce}_{0.8}\text{Sm}_{0.2}\text{O}_{3-x} \cdot x\text{BaCe}_{0.8}\text{Sm}_{0.2}\text{O}_{3-x}$  ( $x=0.1$  mole fraction) measured under open circuit condition at 700°C is shown in Table.4. The highest conductivity of  $1.19 \times 10^{-3} \text{ Scm}^{-1}$  is observed for the composite sintered at 1400°C for 20 minutes using microwave techniques. Hence microwave sintering can be an effective technique for the development of dual phase SDC-BCS microstructure in Ba10CS composite in less processing time. Hence, SDC-BCS composite electrolyte with dual matrix can give the required ionic conductivity operated at intermediate temperature for solid oxide fuel cell applications [27,31].

## Conclusions

SDC-BCS composite is successfully synthesized by co precipitation method and followed by microwave sintering. The presence of both the phase confirms the obtained green powder is a composite one. The phase formation temperature of both doped ceria (SDC) and doped barium cerate (BCS) phases are identified through thermal analysis and found to be 900°C. Such low calcination temperature is possible because of chemical reaction occurred at atomic level. The average particle size for SDC-BCS powder varies from 20-27 nm. The structural analysis confirms the existence of both SDC and BCS phase. The crystal structure is found to be cubic fluorite and orthorhombic perovskite phase respectively for SDC and BCS Phase. The morphology of the composite is free from pores and both the phases are homogeneously distributed. The increase in conductivity is due to the diffusion of oxygen ion preferred to migrate through the continuous channel of samarium doped barium cerate phase. Hence, the SDC-BCS composite with dual phase microstructure can act as a best choice of electrolyte for the energy conversion in solid oxide fuel cell application.

## References

1. S.C. Singhal, *Solid state ionics*. 135 (2000) 305.
2. D.J.L. Brett, A. Atkinson, N.P. Brandon, S.J. Skinner, *Chem. Soc. Rev.* 37 (2008) 1568.
3. J. Garcia-Barriocanal, A. Rivera-Calzada, M.Varela, Z. Sefroui, E. Iborra, C. Leon, S.J. Pennycook, Santamaria, *J. Science*. 321 (2008) 676.
4. B.C.H. Steele, *Solid State Ionics*.129 (2000) 95.

5. M. Goedickemeier, L.J. Gauckler, *J. The Elect. Society*.145 (1998) 414.
6. J. Luo, R. J. Ball, R. Stevens, *J.Materials Science*. 39 (2004) 235.
7. Haile, M. Sossina, *Acta Materialia*.51 (2003) 5981.
8. H. Kato, T. Kudo, H.Naito, H.Yugami, *Soild State Ionics*.159 (2003) 217.
9. T. Takahashi, H. Iwaha, *J.Energy Conversion*. 1 (1971) 105.
- 10.K.D. Kreuer, *Solid state ionics*. 97 (1997) 1.
11. D. Shima, S.M. Haile, *Solid State Ionics*. 97 (1997) 443.
12. T. Mahata, G. Das, R.K.Mishra, B.P.Sharma, *J. Alloys and Compounds*. 391, (2005) 129.
13. A.Venkatasubramanian, P.Gopalan, T.R.S.Prasanna, *J.Hydrogen energy*. 35 (2010)4597.
14. W. Sun, Y.Jiang, Y.Wang, S.Fang, Z.Zhu, W.Liu, *J.Power Sources*. 196 (2011) 62.
15. C.J. Bardwell, R.I.Bickley, S.Poulston, M.V.Twigg, *J.Thermochimica Acta*. 613 (2015) 94.
16. T.S. Zhang, J.Ma, L.B.Kong, P.Hing, J.A.Kilner, *Solid State Ionics*.167 (2004) 191.
17. K.C. Anjaneya, G.P.Nayaka, J.Manjanna, V.M.Ashwin Kumar, G.Govindaraj, K.N.Ganesha, *J.Alloys and Compounds*.598 (2014) 33.
18. J.G. Li, Y.Wang, T.Ikegami, T.Mori, T.Ishigaki, *J.Mat. Sci. and Engineering: B*.121 (2005) 54.
19. S.U. Dubal, A.P.Jamale, S.T.Jadhav, S.P.Patil, C.H.Bhosale, L.D.Jadhav, *J.Alloys and Compounds*.587 (2014) 664.
20. K.S. Knight, *Solid State Ionics*.74, 3-4 (1994) 109.
- 21 A.J. Jacobson, B.T. Tofield, B.E.F. Fender, *Acta Crystallographica Section B: Structural Crystallography and Crystal Chemistry*. 28 (1972) 956.
22. S.T. Jadhav, V.R. Puri, L.D.Jadhav, *J. Alloys and Compounds*. 685 (2016) 626.
23. H. Wang, L. Zhang, X.Liu, H Bi., S.Yu, Han F., Pei L., *J.Alloys and Compounds*. 632 (2015) 686.
24. S.M. Haile, D.L. West, J.Campbell, *J.Materials Research*.13 (1998) 1576.
25. J. Maier, *Nature materials*. 4 (2005) 805.
26. W. Sun, W. Liu, *J. Power Sources*. 217 (2012) 114.
27. Q.X. Fu, S.W.Zha, W.Zhang, D.K.Peng, G.Y.Meng, B.Zhu, *J. Power Sources*. 104 (2002) 73.
28. A.S. Kumar, R. Balaji, S. Jayakumar, C.Pradeep, *J. Mater Chem. Phys*. 182 (2016) 520.
29. P. Gupta, D. Kumar, M.A. Quraishi, O. Parkash, *J. Mater. Env. Sci*. 6(1) (2015) 155.
30. P. Garg, P. Gupta, D. Kumar, O. Parkash, *J. Mater. Env. Sci*. 7 (5) (2016) 1461.
31. N. Singh, R. Mazumder, P. Gupta, D. Kumar, *J. Mater. Env. Sci*. 8 (2017) 1654.

(2018) ; <http://www.jmaterenvirosci.com>